

Nanostructured tool steel fabricated by combination of laser melting and friction stir processing

Y. Morisada^{c,*}, H. Fujii^a, T. Mizuno^b, G. Abe^b, T. Nagaoka^c, M. Fukusumi^c

^a Joining and Welding Research Institute, Osaka University Ibaraki, Osaka 567-0047, Japan

^b AMC Corporation, Konohana-ku, Osaka 554-0024, Japan

^c Osaka Municipal Technical Research Institute Joto-ku, Osaka 536-8553, Japan

ARTICLE INFO

Article history:

Received 7 July 2008

Received in revised form 4 November 2008

Accepted 11 November 2008

Keywords:

Friction stir processing

Laser melting

Tool steel

Microstructural refinement

Pinning effect

Hardness

ABSTRACT

The microstructural control of tool steel (SKD11) by laser melting and friction stir processing (FSP) was studied. A nanometer-sized microstructure consisting of fine M_7C_3 carbide (particle size: ~ 100 nm) and a matrix (grain size: ~ 200 nm) was successfully fabricated by the FSP on the laser treated SKD11. The nanostructured SKD11 had an extremely high hardness of about 900 HV even with its relatively high amount of retained austenite.

© 2008 Elsevier B.V. All rights reserved.

1. Introduction

Tool steels are indispensable materials in various industrial fields, and are used for cutting tools, dies, molds, and so on. Tool steels have been developed through the addition of large amounts of alloying elements in order to disperse many carbide particles in iron based matrix. However, the improvement of mechanical properties, such as hardness, by the compositional modification has become limited. Furthermore, the amount of alloying elements should be reduced because of resource savings, cost reduction, and recyclability requirements.

Recently, much attention has been paid to structural refinement, which improves the mechanical properties of metallic materials. It is well known that the grain refinement of the matrix increases strength and hardness in accordance with the Hall–Petch relation. Several severe plastic deformation (SPD) processes have been developed to reduce the grain size of various metallic materials [1–4]. However, the grain refinement of tool steels by a representative SPD process, such as Equal-Channel Angular Pressing (ECAP) and Accumulative Roll Bonding (ARB), is quite difficult because of the high deformation resistance of tool steels. Compared with other SPD processes, friction stir processing (FSP), which is the same tech-

nique as friction stir welding (FSW), can be easily used for various metallic materials [5–9]. A selected area of a metal plate could be modified by a rotating tool which is inserted into the metal plate, hence producing a highly plastically deformed zone. The stir zone consisting of fine and equiaxed grains has excellent strength and hardness [10,11].

Additionally, the uniform dispersion of the fine carbide particles is also important for increasing its mechanical properties as well as helping to extend the lifetime of various steel parts. Though the exfoliation of the large carbide particles leads to serious defects, that of the nanometer-sized carbide particles is negligible for general applications. Usually, the coarse carbide particles with particle sizes of several tens of micrometers are dispersed in the matrix of tool steels. It is difficult to refine the carbide particles by only the FSP because of their high hardness and thermal stabilities. In this study, the microstructural control of tool steel by the combination of laser melting and FSP is investigated in order to form a nanometer-sized microstructure.

2. Experimental procedure

A commercially available plate of tool steel (SKD11) was used in this study. The chemical composition of the SKD11 is shown in Table 1. The surface of the plate was melted by multi-pass laser heating (1 kW, LASERLINE LDF-1000–750) to produce a rapidly solidified zone for the FSP. The scanning rate of the laser beam and

* Corresponding author. Tel.: +81 6 6963 8157; fax: +81 6 6963 8145.
E-mail address: morisada@omtri.city.osaka.jp (Y. Morisada).

Table 1
Chemical composition of the as-received SKD11.

C	Si	Mn	P	S	Cu	Cr	Mo	V
1.48	0.29	0.35	0.25	0.01	0.09	11.74	0.85	0.22

(Unit: mass %).

the beam diameter at the surface of the plate were 1000 mm/min and 1 mm, respectively. The overlap between the pass of the beam was 0.3 mm. The as-received SKD11 and the laser treated SKD11 were modified by the FSP. The FSP was completely carried out in the rapidly solidified zone of the laser treated SKD11. The FSP tool made of hard metal (tungsten carbide based alloy) had a columnar shape ($\varphi 12$ mm) with a probe ($\varphi 4$ mm, length: 0.5 mm). No detectable chips and cracks were found on the surface of the tool after the FSP by optical microscopy observation. A constant tool rotating rate of 400 rpm was adopted and the constant travel speed was 400 mm/min. A tool tilt angle of 3° was used. The microstructural control process by the laser melting and the FSP is illustrated in Fig. 1.

Transverse sections of the as-received and treated SKD11 were mounted and then mechanically polished. The distribution and the size of the carbide particles were first observed by optical microscopy. The particle size of the carbide and the grain size of the matrix were then evaluated by TEM (JEOL JEM-2100). The chemical composition of the carbide particle was measured by

STEM-EDS (JEOL EM-24511SIOD, JED-2300). The crystal structures of the matrix and the carbide particles were identified by XRD (Rigaku RINT2500 V). The microhardness was measured using a micro-vickers hardness tester (Akashi HM-124) with a load of 300 g.

3. Results and discussion

3.1. Microstructure of the laser treated SKD11

The rapidly solidified zone fabricated by the laser melting could be clearly confirmed in Fig. 2(a). The unique shape of the zone was formed by the laser lapping. There were many coarse carbide particles in the matrix of the as-received SKD11 as shown in Fig. 2(b). On the other hand, no coarse carbide particles could be confirmed in the rapidly solidified zone. The carbide formed a fine dendritic structure as shown in Fig. 2(c). The microhardness was increased from 260 to 473 HV by the microstructural change from the annealed structure to the rapidly solidified structure. Fig. 3 shows TEM images of the dendritic carbide. The dendritic structure consisted of fine carbide particles with a size less than $1 \mu\text{m}$. It is considered that the carbide particles were crystallized on the grain boundary during the rapid solidification. Fig. 4 shows an STEM image and element mapping data of chromium and iron in the carbide. The correlation of the STEM image and the distribution of chromium suggest that the particle is basically chromium carbide.

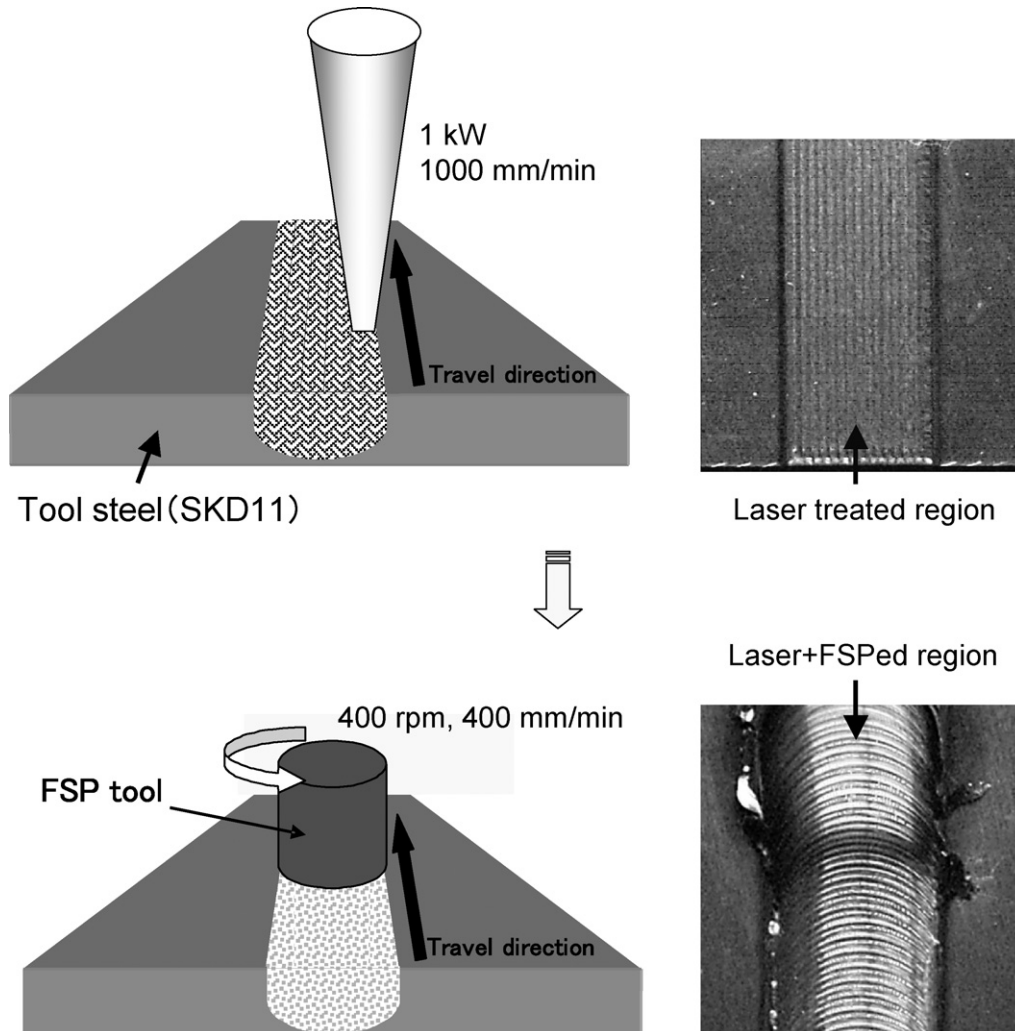


Fig. 1. Schematic of the microstructural control by the laser melting and the FSP.

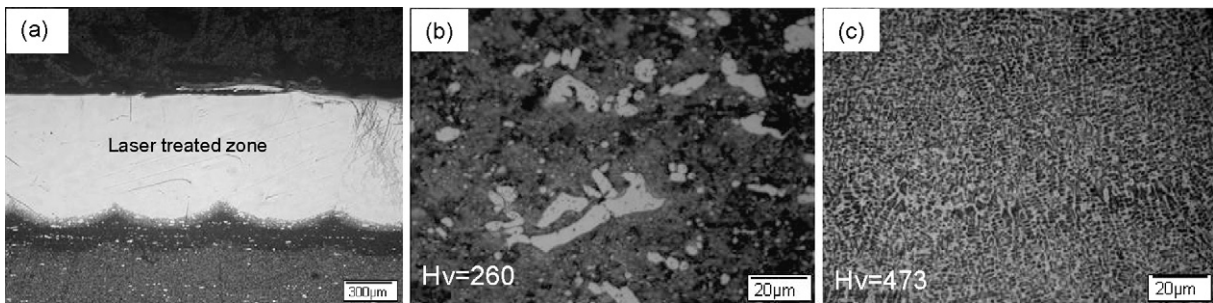


Fig. 2. OM images of (a) cross section of the laser treated SKD11, (b) enlarged image of the untreated zone, and (c) enlarged image of the rapidly solidified zone.

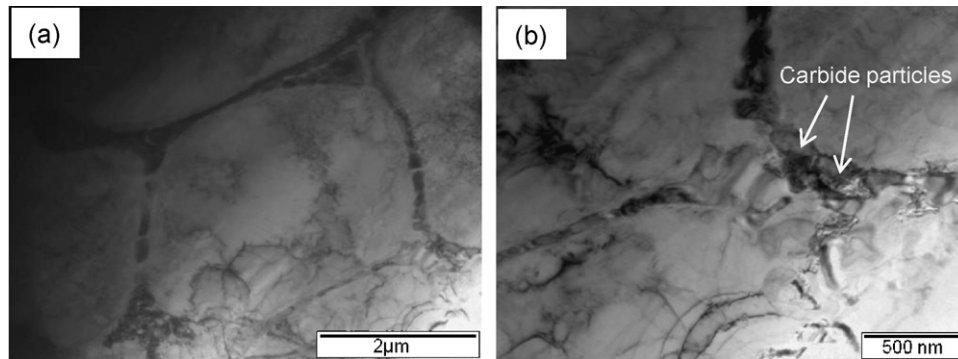


Fig. 3. TEM images of (a) dendritic carbide structure and (b) enlarged image of (a).

3.2. Nanostructured SKD11 fabricated by the combination of the laser melting and the FSP

Fig. 5 shows a cross section of the SKD11 treated by the combination of the laser melting and the FSP. The structures were completely different among the untreated zone, the laser treated zone and the Laser + FSPed zone. There were no coarse carbide particles and dendritic carbide structure in the FSPed zone as shown in Fig. 6(a). The carbide particles and the grains of the matrix became much smaller with sizes ~ 100 and ~ 200 nm, respectively. The authors have studied the grain refinement of various metals by the FSP and found that the FSP with small reinforcements, such as SiC particles, MWCNTs, and fullerenes, more effectively made the grains finer due to the enhancement of the induced strain and the pinning effect during the FSP [12–15]. In this study, the fine carbide particles formed by the laser melting played the same role. The carbide particles were smashed by the rotating tool during the FSP. Additionally, the segregated carbide particles were uniformly dispersed by the fric-

tion stirring. However, it is difficult to fabricate the nanostructural SKD11 without laser melting. Fig. 7 shows the microstructure of the FSPed SKD11 without laser melting. Several coarse carbide particles, which were about $10 \mu\text{m}$ in size could be confirmed as shown in Fig. 7(a). The size of the well refined carbide particles was also relatively coarser compared to the SKD11 treated by the combination of laser melting and FSP as shown in Fig. 7(b).

Fig. 8 shows the XRD patterns of the as-received and the variously treated SKD11s. The main microstructural constituent of the treated SKD11 was found to be martensite. In particular, there was no peak of austenite in the FSPed SKD11 without laser melting. On the other hand, a relatively large amount of retained austenite was confirmed in the laser melted SKD11, regardless of the FSP. It is considered that the austenite was stabilized by the solution of carbon and chromium in the matrix by laser melting. The carbide was identified as the M_7C_3 type in all samples. The peak attributed to the carbide formed by laser melting was shifted to a high angle as shown in Fig. 9. The peak shift indicated that the carbide was

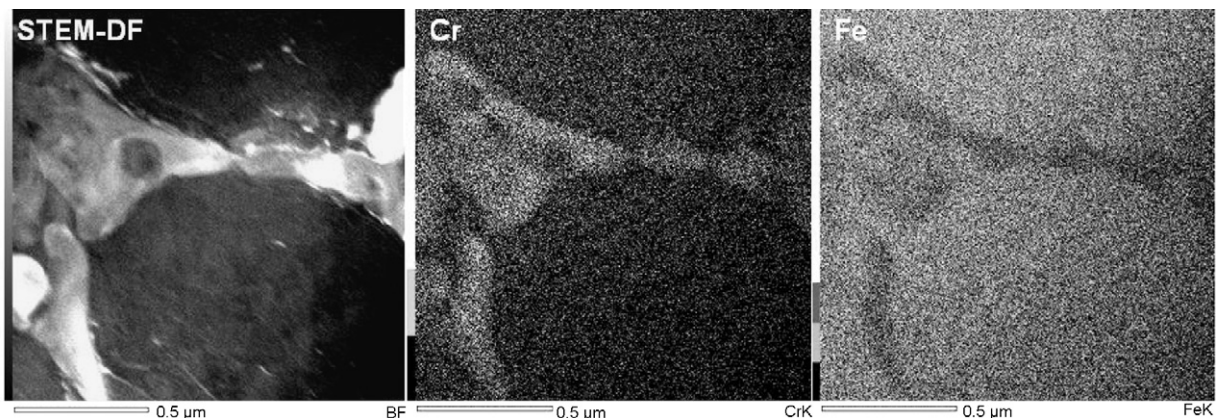


Fig. 4. STEM image and element mappings of the dendritic carbide structure.

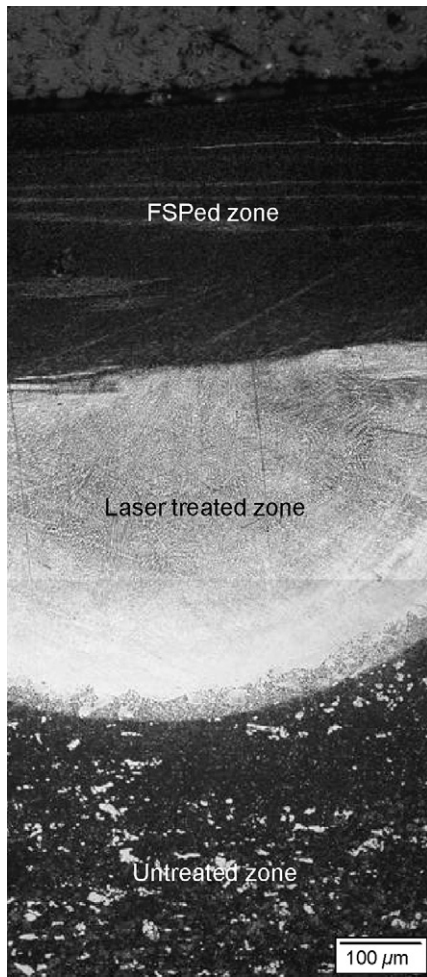


Fig. 5. OM image of the cross section of the SKD11 treated by the combination of the laser melting and the FSP.

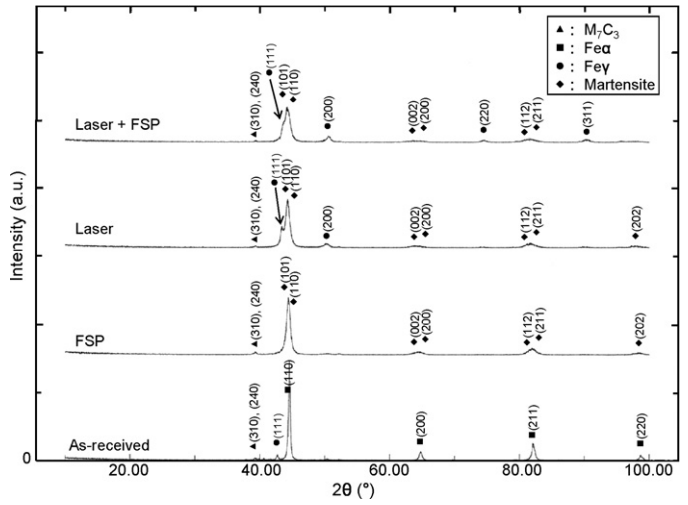


Fig. 8. XRD patterns of the as-received SKD11 and the various treated SKD11s.

Table 2
Chemical composition of the carbides measured by STEM-EDS.

	C	Cr	Fe	Mo
FSP	45.82	30.56	23.16	0.46
Laser	46.90	21.66	30.18	1.26
Laser+FSP	37.60	26.28	33.44	2.68

(Unit: at %).

melted during the laser process and captured metal elements, such as iron and molybdenum, from the matrix. The composition of the carbide measured by STEM-EDS supports the XRD results as listed in Table 2.

The microhardness depth and horizontal profiles for the treated SKD11 are shown in Fig. 10 and 11, respectively. The microhardness at 0.25 mm from the surface was measured for the horizontal profile. The SKD11 treated by the combination of laser melting and the FSP, notwithstanding its large amount of retained austenite, had a

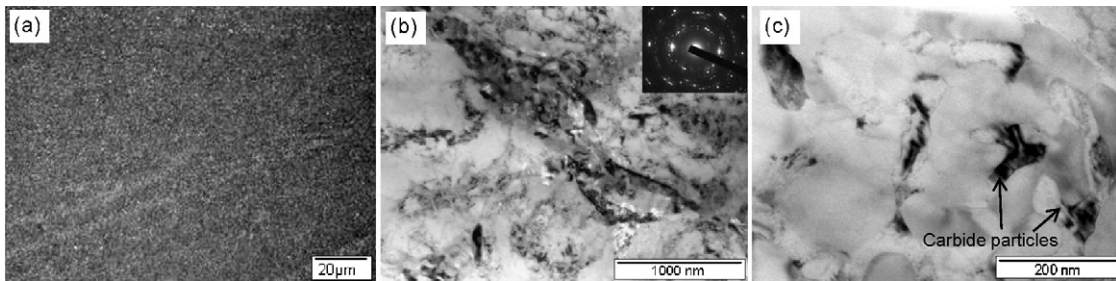


Fig. 6. Microstructure of the SKD11 treated by the combination of the laser melting and the FSP. (a) OM image, (b) TEM image, and (c) enlarged image of (b).

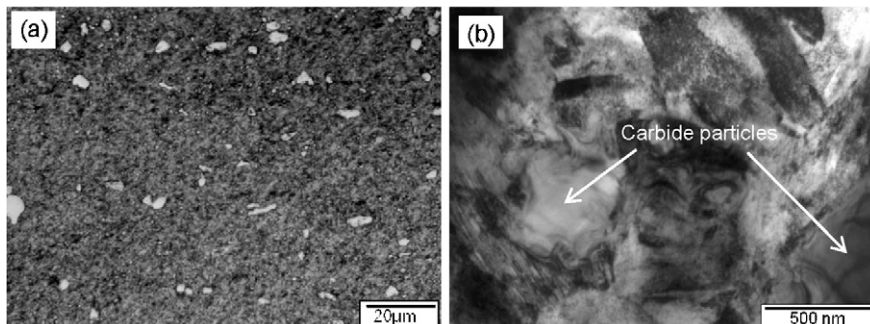


Fig. 7. Microstructure of the FSPed SKD11 without the laser melting. (a) OM image and (b) TEM image.

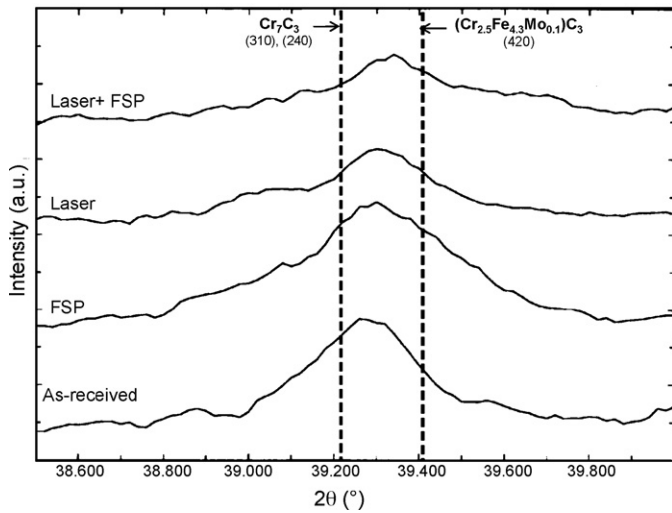


Fig. 9. XRD patterns of the carbides.

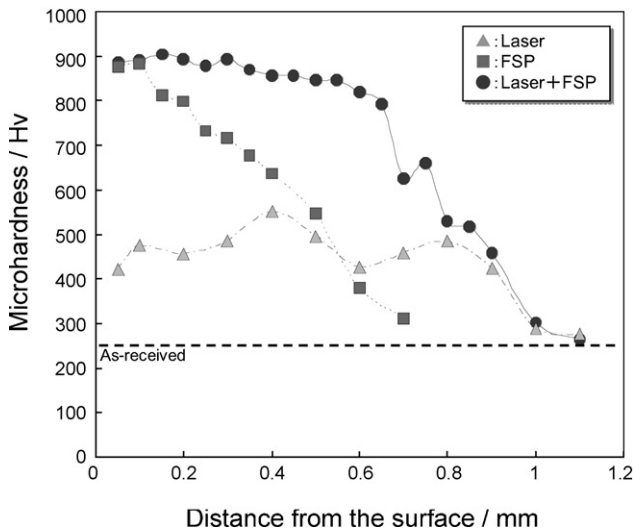


Fig. 10. Microhardness depth profiles of the cross section of the as-received SKD11, the laser treated SKD11, the FSPed SKD11, and the SKD11 treated by the combination of the laser melting and the FSP.

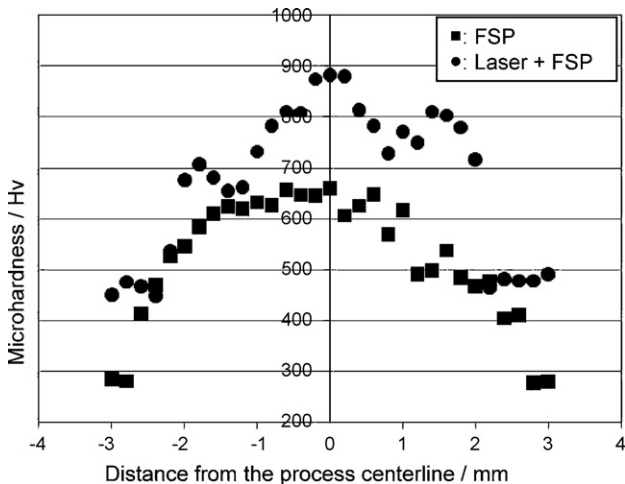


Fig. 11. Microhardness horizontal profiles of the cross section of the FSPed SKD11, and the SKD11 treated by the combination of the laser melting and the FSP.

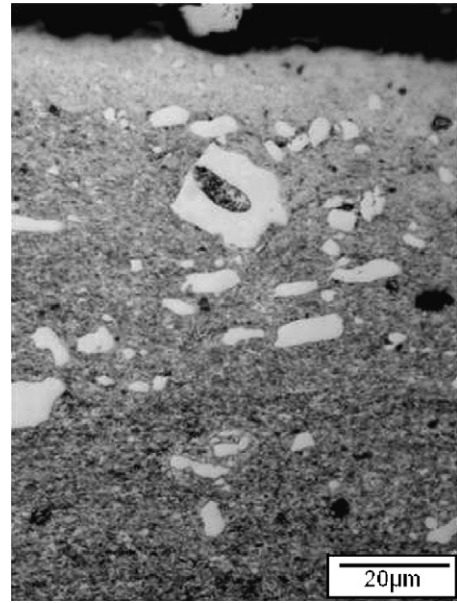


Fig. 12. OM image of the carbides accumulation near the surface of the FSPed SKD11.

large area with an extremely high hardness of about 900 HV which should be the highest hardness possible for the SKD11. It is considered that the nanostructure consists of fine grains of the matrix (grain size: ~200 nm) and well distributed fine carbide particles (particle size: ~100 nm) that led to such a high hardness. Usually, the toughness and corrosion resistance of the austenite is better than those of the martensite. The SKD11 treated by the combination of the laser melting and the FSP seems to be a suitable material for various parts which are used under severe conditions. Though the hardness of the FSPed SKD11 was similar to that of the FSPed SKD11 with the laser melting near the surface, it should be reflected by the formation of the martensite and the accumulation of the coarse carbide particles which were blown up by the plastic flow during the FSP as shown in Fig. 12.

Figs. 11 and 12.

4. Conclusions

The matrix grains and carbide particles of the SKD11 were significantly refined by the laser melting and the FSP. The microstructure and microhardness were evaluated by observations of the grain size and phase of the matrix, and the size and dispersion of the carbide particles. The obtained results can be summarized as follows.

The nanometer-sized microstructure consists of a fine carbide (particle size: ~100 nm) and matrix (grain size: ~200 nm) as fabricated by the combination of laser melting and the FSP.

The carbide is the M_7C_3 type for the FSPed SKD11 with and without laser melting. The carbide formed by laser melting includes a high amount of iron and molybdenum when compared to that formed by the FSP without laser melting.

The microstructural constituent of the laser treated SKD11 with and without the FSP is martensite and the retained austenite.

The nanostructured SKD11 has an extremely high hardness of about 900 HV even with its relatively high amount of retained austenite.

Acknowledgements

The authors wish to acknowledge the financial support of a Grant-in-Aid for Young Scientists (B) and a Grant-in-Aid for Science Research (B) from the Ministry of Education, Culture, Sports, Science and Technology.

References

- [1] R.Z. Valiev, N.A. Krasilnikov, N.K. Tsenev, *Mater. Sci. Eng. A* 137 (1991) 35.
- [2] M. Furukawa, Z. Horita, M. Nemoto, R.Z. Valiev, T.G. Langdon, *Acta Mater.* 44 (1996) 4619.
- [3] Y. Saito, N. Tsuji, H. Utsunomiya, T. Sakai, R.G. Hong, *Scripta Mater.* 39 (1998) 1221.
- [4] N. Hansen, X. Huang, R. Ueji, N. Tsuji, *Mater. Sci. Eng. A* 387–389 (2004) 191.
- [5] K. Ohishi, T.R. Mcnelley, *Metall. Trans. A* 35A (2004) 2951–2961.
- [6] J.Q. Su, T.W. Nelson, C.J. Sterling, *Scripta Mater.* 52 (2005) 135–140.
- [7] D.C. Hofmann, K.S. Vecchio, *Mater. Sci. Eng. A* 402 (2005) 234–241.
- [8] H.J. Liu, H. Fujii, K. Nogi, *Mater. Sci. Tech.* 20 (2004) 399–402.
- [9] H. Fujii, Y.G. Kim, T. Tsumura, T. Komazaki, K. Nakata, *Mater. Trans.* 47 (2006) 224–232.
- [10] K.V. Jata, S.L. Semiatin, *Scripta Mater.* 43 (2000) 743–749.
- [11] S.H.C. Park, Y.S. Sato, H. Kokawa, *Scripta Mater.* 49 (2003) 161–166.
- [12] Y. Morisada, H. Fujii, T. Nagaoka, M. Fukusumi, *Mater. Sci. Eng. A* 433 (2006) 50–54.
- [13] Y. Morisada, H. Fujii, T. Nagaoka, M. Fukusumi, *Mater. Sci. Eng. A* 419 (2006) 344–348.
- [14] Y. Morisada, H. Fujii, T. Nagaoka, M. Fukusumi, *Scripta Mater.* 55 (2006) 1067–1070.
- [15] Y. Morisada, H. Fujii, T. Nagaoka, K. Nogi, M. Fukusumi, *Composites A* 38 (2007) 2097–2101.